We are IntechOpen,
the world's leading publisher of
Open Access books
Built by scientists, for scientists

6,400
Open access books available

174,000
International authors and editors

190M
Downloads

Our authors are among the

154
Countries delivered to

TOP 1%
most cited scientists

12.2%
Contributors from top 500 universities

BOOK CITATION INDEX
CLARIVATE ANALYTICS
INDEXED

WEB OF SCIENCE™

Selection of our books indexed in the Book Citation Index
in Web of Science™ Core Collection (BKCI)

Interested in publishing with us?
Contact book.department@intechopen.com

Numbers displayed above are based on latest data collected.
For more information visit www.intechopen.com

Chapter

Characterization of Degraded Cartilage Using Confocal Raman Microscopy

N'Dre Jean, Hamideh Salehi, Marie Maumus, Danièle Noël, Yolande Koffi-Gnagne and Frédéric Cuisinier

Abstract

Osteoarthritis is a degenerative disease with pathological changes at the molecular level. Moreover, the damage to articular cartilage is irreversible. Early detection and the ability to follow the progression of osteoarthritis are essential to anticipate management. To characterize degraded human articular cartilage and to identify cellular changes that are precursors of phenotypic matrix changes in osteoarthritis, normal and degraded articular cartilage explants were harvested from the same patient's knee after informed consent. The blocks were washed several times (four times) with phosphate-buffered saline (often abbreviated to PBS) and then fixed on CaF2 slides using Cell-Tak® (an adhesive glue), and the whole set was placed in different Petri dishes containing PBS for Raman measurements. The analysis of the spectroscopic data allowed to differentiate degraded cartilage from normal cartilage by applying intensity ratios of some Raman bands and/or spectral regions. In addition, peaks at 864, 929, 945, 1107, 1386, and 2887 cm^{-1} were identified as characteristic Raman markers of degraded cartilage. The use of confocal Raman microscopy (CRM) has proven to be relevant in providing biochemical information necessary to characterize OA cartilage. CRM appears to be a powerful tool for the diagnosis and therapeutic evaluation of osteoarthritis in both early and late stages.

Keywords: articular cartilage, osteoarthritis, confocal Raman microscopy

1. Introduction

Osteoarthritis (OA) is the most common degenerative joint disease and one of the main causes of morbidity and economic burden for health resources. It is a slowly progressive disease that alters all tissues of the affected joint, with a long asymptomatic period [1]. According to OARSI (International Association for the Study of Osteoarthritis), OA is a serious disease defined as a disorder involving mobile joints, characterized by adhesive stress and degradation of the extracellular matrix, resulting in macro- and micro-damage that activates abnormal adaptive restorative responses, including pro-inflammatory pathways of the immune system [2]. Emerging evidence in recent years defines OA as a heterogeneous, multifaceted disease with multiple

molecular and clinical phenotypes [3, 4]. Loss of articular cartilage structure and function is one of the main features of OA [5–7].

The current diagnosis of OA is based primarily on radiographic criteria (e.g., joint space width, osteophyte formation, subchondral sclerosis) and clinical symptoms (e.g., pain, stiffness, and loss of function). Radiography is the most accessible tool for assessing OA: It can show lesions and other changes related to OA to confirm its severity according to different classification systems, such as Kellgren's Lawrence classification system [8]. MRI, which does not use radiation, is more expensive than X-rays but can provide better images of cartilage and other structures to detect early abnormalities in OA [9]. Another imaging technique is optical coherence tomography (OCT) imaging, which has the ability to generate cross-sectional images of articular cartilage and can provide quantitative information about the condition of articular cartilage, particularly for OA caused by changes in collagen structure [10]. Although these different medical tests are more sensitive than plain radiography, they cannot be routinely applied to many patients due to its cost, and if so, they are often time-consuming and even destructive. The other disadvantage is that these techniques are only valid and feasible in the advanced stages of osteoarthritis.

Currently, the lack of validated biomarkers and early diagnostic tools is one of the major obstacles to improved diagnosis and therapeutic evaluation of OA [11]. Recently, Raman spectroscopic techniques have been shown to not only provide noninvasive and nondestructive structural information in damaged cartilage, but also to allow spatial resolution at the biomolecular level that can be useful in detailed structural analyses of cartilage diseases. Indeed, these techniques can identify functional groups and chemical bonds present in biological tissues and/ or cells. As a result, it is possible not only to assess the structure of proteins, lipids, carbohydrates, and nucleic acids present in a biological molecule [12–15], but also the changes in their chemical structure due to the disease process [3, 11], thus allowing monitoring of the progression of the disease process and prediction of the chemical pathway of the progression. Vibrational spectroscopy thus appears to be a proven analytical tool for understanding chemical changes associated with pathological conditions in tissues. The objective of our study was to characterize degraded human articular cartilage using confocal Raman microscopy (CRM) and to identify early cellular changes that are precursors to the phenotypic change of the matrix in OA.
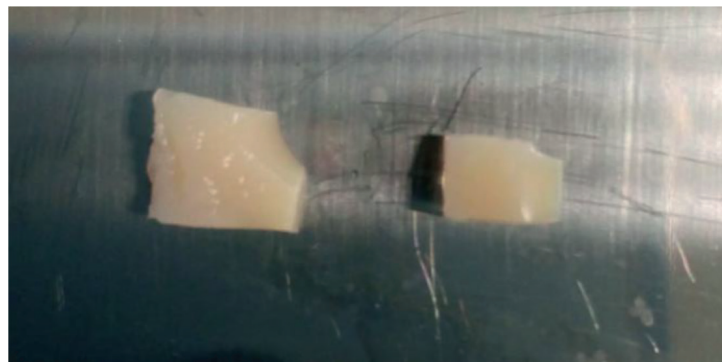
Figure 1.
*Cartilage samples taken from a patient's knee.*

2. Materials and methods

2.1 Source and preparation of samples

Our samples consisted of human articular cartilage explants taken from the knee of one patient (**Figure 1**). The biopsies were taken from the same knee but at different locations. For example, degraded cartilage (test sample) at the lesion site and normal cartilage (control sample) away from the lesion site. Human tissue was obtained for research purposes with donor consent. The study was also approved for the recovery of OA samples by the Ministry of Research and Innovation and the Comité d'Éthique de la Protection des Données Personnelles (CPP) of Languedoc-Roussillon (approval DC-2010-1185). The cartilage samples were collected from the same patient. The collected sample blocks were washed several times (four times) with phosphate-buffered saline (often abbreviated to PBS) and then fixed on CaF2 slides using Cell-Tak® (adhesive glue). The whole set was placed in different Petri dishes containing PBS for Raman measurements. During the whole measurement period, the samples were kept in a refrigerator at 4°C.

2.2 Raman measurements of the samples

All measurements were performed using a Witec α 300R confocal Raman microscope (Witec, Ulm, Germany) (**Figure 2a**). The system was equipped with a dual-frequency Nd: YAG laser (Newport, Evry, France) with a wavelength of 532 nm and a NIKON × 20 aerial lens with a numerical NA of 0.46 (Nikon, Tokyo, Japan). The output laser power was 50 mW. The spatial resolution was 300 nm, and the depth resolution was approximately 1 μm. The microscope was equipped with a piezo-driven scanning stage with a positioning accuracy of 2–3 nm horizontally and 10 nm vertically, respectively. The acquisition time for a single spectrum was set to 0.5 s; 150 × 150 points per image were recorded, resulting in a total of 22,500 spectra for one image. Data acquisition was performed using Image Plus 2.08 software from Witec. Using an edge filter, the backscattered Raman radiation was

(a)   (b)
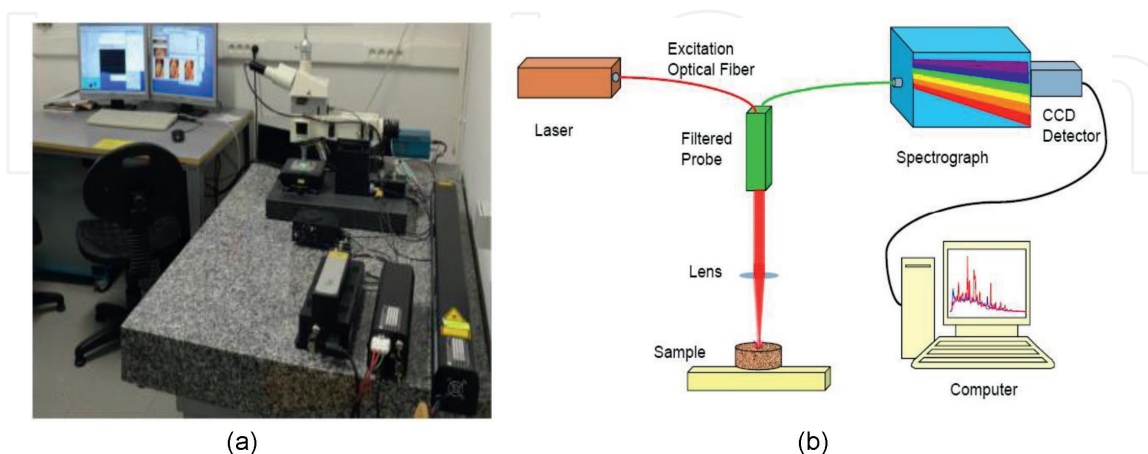
Figure 2.
Measurement of articular cartilage using confocal Raman microscopy. (a) Confocal Raman microscope at Laboratoire Bioingénierie et nanoscience UM_104 Montpellier. (b) Schematic representation of the system. The laser light source irradiates the articular cartilage, and the scattering light is generated by the scattering of the samples. The Raman scattering light is obtained by the filter, and the Raman spectrum is presented after its detection and processing by a CCD detector. The data of the spectra are analyzed using multivariate or chemometric methods.

separated from the scattered Rayleigh light. The Raman photons were transferred to the EMCCD camera (DU 970 N-BV353, Andor, Hartford, USA). The EMCCD chip size is 1600 × 200 pixels, the camera controller is a 16-bit A/D converter operating at 2.5 MHz, and the camera is cooled by a Pelletier system. The UHTS 300 spectroscopy system with 70% transmission and a 600 lines per mm grating (operating at ‑60° C) provides a spectral resolution of 3–5 cm^{-1}. This microscope was used for the analysis of articular cartilage structures.

2.3 Analysis of the Raman spectral data

All collected spectra were preprocessed in order to obtain spectra that not only have the same scale, but are comparable to each other. The spectral analysis was performed in the fingerprint range (600–1800 cm^{-1}) due to its higher molecular specificity. Prior to the multivariate statistical analysis, the Raman spectra were preprocessed using well-established techniques. The preprocessing process of the spectra consisted, first, of baseline subtraction following the eighth-order polynomial law. Subsequently, we proceeded to the elimination of the autofluorescence of the tissues and the smoothing of the spectra using the "Savitzky Galay" filter, following a polynomial order = 4 with a number of points (or interval = 13). In order to compare the spectra and allow consistent comparisons where intensity variations may be relative to the intensity of each spectrum, the data were normalized to the area of the region between 600 and 1800 cm^{-1} [15]. These steps of preprocessing the spectra were necessary before subjecting them to statistical methods. All preprocessing, normalization, and determination of the different intensities of the peaks or bands were performed with the non-commercial Spectragryph® software version 1.2.12 developed and kindly offered by Dr. Friedrich Menges.

In addition, multivariate analyses such as principal component analysis (PCA) were applied to the raw dataset collected from the different samples. PCA is a well-established multivariate data analysis method that is well suited to distinguish small recurrent spectral variations from large datasets containing uncorrelated variations. It is a completely unsupervised analysis method for establishing whether or not sample spectra are grouped into classes based on sample type among other factors. This method greatly reduces the size of the dataset into a defined number of principal components (PCs), as all spectra are expressed in terms of a few basic functions (usually <10) and "a score vector" of about p entries. Thus, if clustering is observed, there are quantifiable and significant variations in the spectra that can be used to build discriminative algorithms to distinguish between different samples. PCA describes large global changes in composition without any prior knowledge.

3. Statistical analysis

Given that the distribution of our data does not follow a normal distribution, all our statistical analyses were performed using a non-parametric test, namely the Kruskal-Wallis one-way analysis of Variance on Ranks statistical test with p < 0.001 for significance of our results. For comparisons between different areas, the Student-Newman-Keuls statistical test with p-value <0.05 was applied. All our data were processed with SigmaPlot for Windows software version 11.0 Build 11.0.0.77.

4. Results

4.1 Characterization of articular cartilage degradation

From the collected cartilage blocks, a total of 50 Raman spectra were collected at different locations on each normal and degraded cartilage sample. The degraded state of the cartilage was assessed by determining the content of PGs and type II collagen, the main components of the extracellular matrix of cartilage, as reported in previous studies [16]. In **Figure 3**, we can easily see that the content of PGs significantly decreased ($p < 0.001$) in degraded cartilage, with a random coil content, characterized by applying the ratios of the integrated areas of the carbohydrate region ranging from 985 to 1185 cm^{-1} to the amide I region (1601–1776 cm^{-1}) [16], the intensity ratio of the two amide III peaks (1241/1269 cm^{-1}), with the peak 1241 cm^{-1} corresponding to the random coil content = NH2 bending: Random coil Amide III and 1269 cm^{-1} corresponding to the alpha-helix content = NH2 bending: alpha-helix Amide III) [17, 18], respectively.

### 4.2 Multivariate analysis and discrimination of Raman bands involved in articular cartilage degradation

The application of PCA on the raw spectra of the different samples allowed us to discriminate degraded cartilage from normal cartilage. **Figure 4** shows us the average and differential Raman spectra with the characteristic differential Raman bands. Also, analyzing the PCA score plot using CP1 and CP2, as well as that using CP2 and CP3, we find that only CP2 separates the degraded/normal samples (**Figure 5**). The CP2 principal component shows the intense positive charges for the Raman shifts in the degraded cartilage, characterized by the localized peaks, respectively at: 788 cm^{-1} (⁻O-P-O⁻); at 821 cm^{-1} (⁻O-P-O⁻); 867 cm^{-1} (RNA); 886 cm^{-1} (collagen I); 926 cm^{-1} (ν (C-C)); 945 cm^{-1} (ν (C-C) backbone); 972 cm^{-1} (ν (C-C) backbone in RNA); 1107 cm^{-1} (ν (C-O)); 1274 cm^{-1} (Amide III); 1386 cm^{-1} (GAG); 1432 cm^{-1} (CH_2 scissoring); 1480 cm^{-1} (CH deformation); 2887 cm^{-1} (CH_2 stretch); and 2947 cm^{-1} (νas CH_2, lipids, fatty acids). These peaks are the expression of vibrations of nucleic
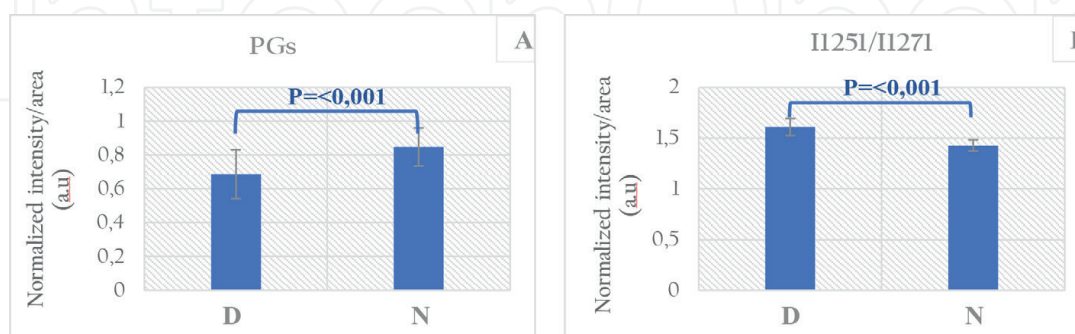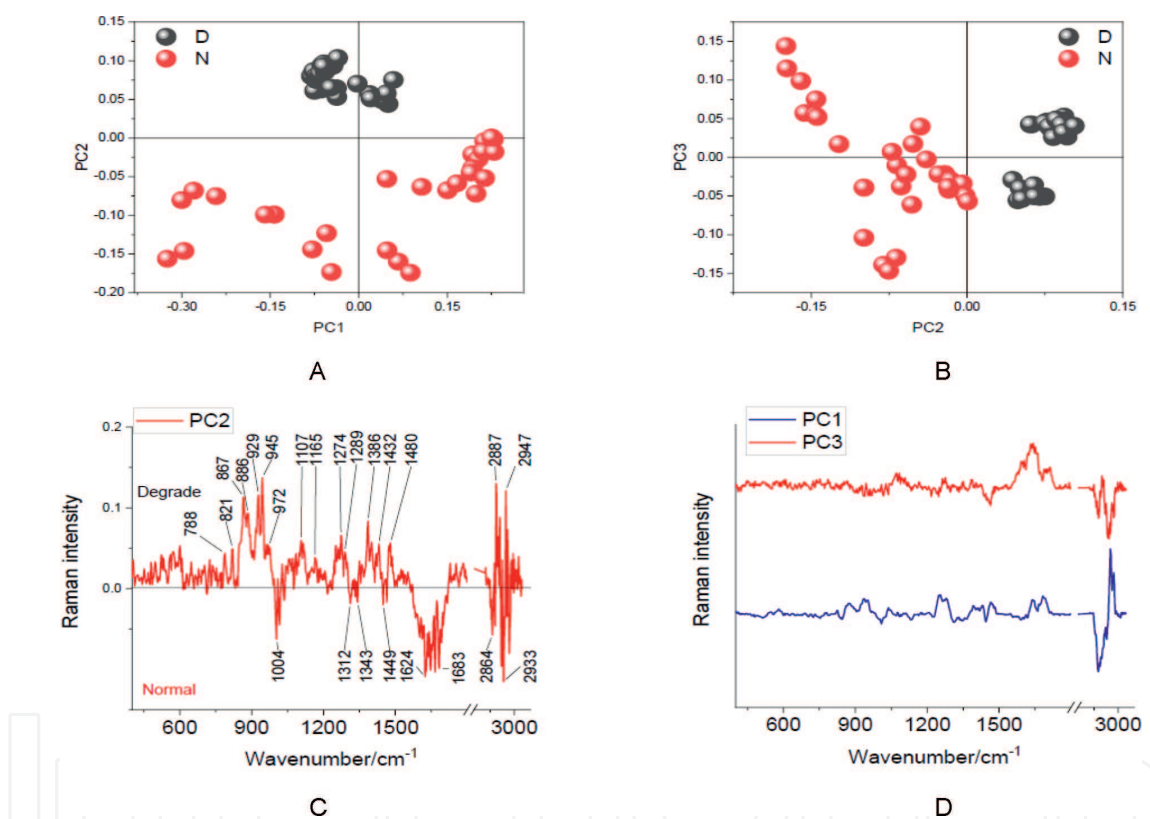

Figure 3.
Characterization of degraded cartilage: (A) determination of PGs content by the ratio of the area of the carbohydrate region [985–1185]/amid region I [1601–1760]. The histogram shows a higher intensity ratio for normal cartilage (CA). This reflects a significant ($p < 0.001$) decrease in PGs in degraded cartilage. (B) The ratio of disordered collagen (random coil) to ordered collagen (α-helix), represented by the intensity ratio I1251/I1271, is significantly greater ($p < 0.001$) and in favor of the random coil in degraded cartilage.
Observations: D: Degraded cartilage; N: Normal cartilage.
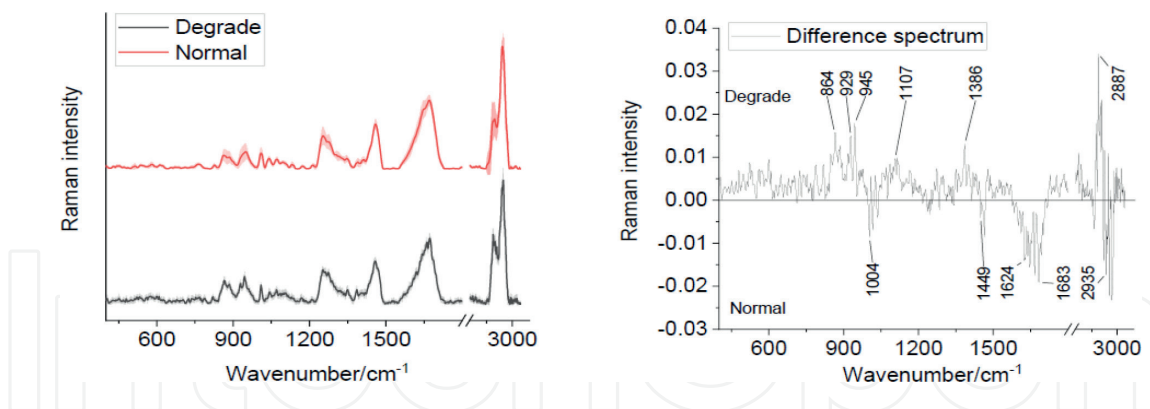
Figure 4.
Average and differential Raman spectra (n = 50 spectra).

Figure 5.
Principal component analysis. (A) PCA score plot using PC1 and PC2. (B) PCA score plot using PC2 and PC3. Only PC2 separates degraded/normal samples. (C) PC2 loading is responsible for separating degraded and normal cartilage samples. (D) Remaining PC1 and PC3 loadings.

acid bases, collagen, and GAGs. In contrast, the negative charge peaks are the characteristic Raman shifts in normal cartilage, reflected in particular by peaks at 1004 cm^{-1} (Phe), 1624 cm^{-1} (Trp), 1683 cm^{-1} (ν (C=O)), and 2933 cm^{-1} (CH$_2$ asymmetric stretch). The assignments of these different peaks are recorded in **Table 1**.

5. Discussion

Pathological changes in cartilage begin at the molecular level (at the nanoscale) from where they propagate to higher levels of the hierarchical cartilage architecture

	Degraded cartilage
Raman shift [cm^{-1}]	Assignments
788	$-O-P-O-$ in DNA
821	$-O-P-O-$ in ARN
867	Collagen, ν (C-C) (Pro), Ribose vibration, one of the distinct modes of RNA (with 915 and 974 cm^{-1})
886	Proteins, including collagen I
926	ν (C-C), stretching - probably in amino acids
945	ν (C-C) backbone
972	ν (C-C) backbone in RNA
1107	ν (C-O), GAG
1165	C, G; Tyrosine (type I collagen)
1274	T, A, Amide III; $=$ CH bending
1289	Phosphodiester group in the nucleic acid
1386	GAG, CH$_3$ band
1432	CH$_2$ shear
1480	G, A; deformation CH (DNA)
2887	Fermi resonance; CH$_2$ stretching
2947	υas CH$_2$, lipids, fatty acids

Table 1.
Table of major Raman peak or band assignments involved in the characterization of degraded versus non-degraded (normal) articular cartilage [12, 17, 19–21].

and cause increasingly irreversible structural and functional damage. Although the etiology of osteoarthritis is largely unknown, its onset is characterized by an imbalance between catabolic and anabolic processes, promoting the degradation of the cartilage matrix. The underlying cause of these macroscopic and microscopic structural features has been linked to the change in biochemical compositions such as alteration and decrease in proteoglycan content but also by the disorganization of type II collagen fibers [18, 22]. The biochemical changes are triggered by the expression of enzymes that are responsible for matrix degradation. The main components of articular cartilage are GAGs (15–30% of dry weight) and collagen (50–60% of dry weight) [23, 24], and their changes can be used as indicators for the early diagnosis of OA. Therefore, any technique to diagnose the onset of OA must detect early changes in cartilage PG gel before significant changes in its collagen matrix occur.

Raman spectroscopy has been shown to provide information on protein structure. Indeed, subtle molecular changes often cause detectable vibrational changes that can be detected by Raman analysis. In recent studies, Raman has been used either to more accurately quantify the distribution of cartilage subcomponents over its entire surface [25] or in some situations to establish the difference between different regions of the tissue over its entire depth the tissue surface [26].

Thus, Raman spectroscopy can be useful in differentiating normal from degraded cartilage. It is now known that the intensity ratio of the two peaks (I1251/I1271 cm^{-1}) provides information about the protein structure [11, 17]. Still called the ratio of

disordered collagen (random coil) to ordered collagen (α-helix), represented by the intensity ratio 1241/1269 cm^{-1}, provides an appreciation of articular cartilage damage [27]. This intensity ratio increases with the progression of osteoarticular diseases following the degree of cartilage damage (ICRS). In the present case, **Figure 3** shows a higher intensity ratio (1251/1271 cm^{-1}) and thus in favor of disordered collagen, characterizing a disordered structure of the protein. This result indicates an increase in defective collagen content. This observation was also made by Kumar et al. [18], who, when analyzing different grades of osteoarthritis, showed that this intensity ratio increased the progression of the cartilage disorder. This alteration of the random coil is associated with a decrease in PGs marking a clear difference between normal and degraded cartilage.

Other more subtle changes were highlighted by the application of PCA, which is a common multivariate statistical method very often used in bioanalytical Raman spectroscopy to reduce dimensionality and identify combinations of the most important spectral markers that maximize data variance and optimize group separation [18]. Indeed, although univariate analysis of Raman intensities in normalized spectra was necessary to differentiate degraded cartilage from normal cartilage by determining proteoglycan and type II collagen contents, multivariate analysis, particularly PCA, has been shown to be very effective in discriminating the two samples and identifying characteristic Raman bands or peaks. This ability of PCA has been widely demonstrated in numerous tissue and cell Raman spectroscopy studies [18, 25].

Figure 5C shows the loadings of the Raman bands responsible for the separation of the degraded and normal cartilage samples. Focusing on the peaks of the degraded cartilage, we find a high nucleotide activity (expressed by the presence of bands at 788, 821, and 1480 cm^{-1}), which could be attributed to the increased internucleosomal DNA cleavage manifested in the advanced stages of OA as revealed also by Verrier et al. [28]. During the progression of ECM degradation, chondrocytes are strongly solicited to renew the matrix proteins subjected to degradation phenomena. This high level of activity can lead to the death of chondrocyte cells by exhaustion, as demonstrated in the work of Zamli et al. [29] after evaluating the role of chondrocyte apoptosis in spontaneous animal models of osteoarthritis. They further demonstrated that chondrocyte death correlated with CA fibrillation (r = 0.3), cellularity< (r = 0.4), proteoglycan depletion, and overall OA microscopic scores (r = 0.4). This supports our results with the depletion of PGs and alteration of type II collagen structure observed in degraded cartilage and characterized by the presence of the high Raman signal intensity peaks at 867, 886, 926, 945 cm^{-1}, and 1274 cm^{-1} (collagen attribution) and peaks at 1107, 1342, and 1386 cm^{-1} (GAGs attribution). Focusing on the 1274 cm^{-1} peak, amide III attribution, Shaikh et al. [30] recently showed significant variations related to the intensity of this band and δCH_2 stretching in a group of cartilage with impact injuries. They therefore inferred that these changes in the intensity of the amide III peak were potentially due to conformational and configurational changes in collagen macromolecules as well as proteoglycan depletion. A first study by Lim et al. [31] had already shown, after an impact on porcine cartilage, a red shift of the 1264–1274 cm^{-1} peak. They correlated this shift of amide III with the compression of the C-N vibration in the collagen fibers. In the case of our study, the presence of the 1274 cm^{-1} peak could therefore reflect an alteration of the random coil associated with the decrease of the PGs content observed above. In addition, the presence of the peak at 1386 cm^{-1}, corresponding to N-acetyl-glucosamine (attribution of hyaluronic acid (HA)), helps to corroborate our observation. It is known that HA constitutes the main skeleton of GAGs. This glycoprotein binds to other aggrecanes to

form superaggregates responsible for tissue hydration, allowing cartilage to respond to mechanical stress. Thus, it helps to organize and stabilize the relationship between PGs and the collagen meshwork. Any changes in this glycoprotein could necessarily lead to disruptions in the structure of the cartilage matrix. As an important component of synovial fluid, HA can increase joint flexibility, thereby reducing cartilage wear. In a study by Buckwalter et al. [32], it could be shown that one of the first changes associated with osteoarthritis and joint immobilization was related to changes in hyaluronic acid glycoprotein. Also, Safiri et al. [33] recently demonstrated that it was associated with the radiological progression of osteoarthritis.

One factor that has also been associated with OA is the appearance of lipid deposits especially in the advanced stages of OA [34]. More recently, Mansfield and Winlove [12] studied the distribution of lipids, identifying two related regions: a band at 1441 cm^{-1} and shifts from 2845 to 2930 cm^{-1}. Generally, the CH vibrational region between 2800 and 3000 cm^{-1} is of particular interest for spectroscopic studies because it provides information about the chemical compositions of the samples due to differences in the C-H bond environment [12, 31]. Thus, it can provide information about the relative total concentration of biomolecules but also about changes in chemical bonds. In a recent study, Gaifulina et al. [35] were able to correlate the alterations observed in cartilage with the loss of tissue constituents and the observed increase in water content. They therefore correlated the observed increase in cartilage hydration with the increase in the intensity of the O-H stretch band. In this study, the Raman shifts of the bands at 2887 and 2947 cm^{-1} (lipid and/or fatty acid vibration) could reflect the strong presence of lipids also in degraded cartilage and explain the possible changes within the cytoplasmic skeleton by lipid production in the face of OA progression. This is justified by the response of chondrocytes to cartilage degradation in order to cope with the physiochemical changes in the cartilage matrix. It should be remembered that lipids are important nutrients in the metabolism of chondrocytes and are available to these cells by *de novo* synthesis, but also by diffusion from the surrounding tissues. Amanda et al. [34], by analyzing the status of cartilage, were able to link the development of osteoarthritis with the availability of lipids. Other more recent studies have reported well-established links with lipid accumulation and the development of OA [36, 37], particularly in its early stages before histological changes occur.

In this study, CRM appears to be very useful in differentiating degraded from healthy articular cartilage tissue. Indeed, during the early stages of osteoarthritis, biochemical changes precede the later structural changes and therefore play a fundamental role in contrast to mechanical factors, which are no longer significant in the advanced stages of disease progression. This makes CRM a privileged tool for early detection of ECM degradation. It is now recognized that CRM can be used for quantitative analysis on thicker, unfixed, hydrated, or even submerged samples, as long as water does not interfere with the Raman signals [13]. Moreover, since depth analysis does not require cutting of the sample, it can be applied to healthy tissue, such as articular cartilage.

In any case, this technique seems to be useful in circumstances where tissue biopsies are recorded or even with Raman-compatible arthroscopic probes [38]. As such, numerous Raman spectroscopy devices in the form of fiber optic probes have been developed and tested for some on human knee joint tissue [39, 40], a common anatomical site for arthroscopic surgery, and allowed detection of cartilage with contributions from subchondral bone [41], others on the colon for real-time *in vivo* assessment of adenomatous polyps [39], or either to nondestructively monitor the

growth of *in vitro* tissue engineering constructs in real time for regenerative medicine applications toward controlled clinical translation [38, 40]. As pointed out by Karen et al. [41], fiber optic probes are a convenient format to couple optical spectroscopies to an arthroscopic probe because they are compatible with the small dimensions of the arthroscope and provide the same chemical information available in a microscopy instrument. In this sense, we agree with Gao et al. [42] that CRM has the potential to be incorporated into a fiber-optic probe device to build a fiber-optic-based confocal Raman microscopy detection unit for an arthroscope for clinical use. As a result, it has the capabilities during arthroscopic procedures to remove the operator from damage to healthy tissue that is usually, in addition to degraded cartilage or sclerotic bone, sometimes included at the microfracture site [41]. Therefore, the coupling of confocal Raman microscopy to arthroscopy could facilitate not only to specifically identify degraded or damaged tissues, but also to better guide surgical interventions by avoiding surrounding healthy tissues. Obviously, such a technology practiced on a daily basis in the clinical setting would strongly contribute to prevent irreversible cartilage damage in the more advanced stages and would favor the institution of adequate management either by stem cell injection to induce regeneration of damaged sites or by other therapeutics without impacting surrounding healthy tissue.

6. Conclusion

Osteoarthritis is a degenerative disease that primarily affects articular cartilage and related joint tissues and imposes an increasing social burden due to overall activity limitation, especially in the elderly. With degradation, the major components of the cartilage ECM, particularly collagen and proteoglycans, are progressively degraded by the released inflammatory factors. Currently, the diagnosis of OA relies on radiographic methods based on the Kellgren-Lawrence scores, in which joint space narrowing is considered the main diagnostic indicator of advanced disease. One of the major challenges in the management of OA is the ability to make an early diagnosis. To date, there are no biomarkers available for early diagnosis of the disease and no effective therapy other than symptomatic treatment and joint replacement surgery.

The results of our study demonstrate the ability of CRM to differentiate damaged from healthy articular cartilage tissue and thus introduce RCM as a future diagnostic tool for the efficient management of OA. The application of CRM has proven to be relevant in providing biochemical information needed to characterize OA cartilage. Combined with multivariate analysis, CRM is able to identify biomarkers to characterize biochemical and structural changes in articular cartilage ECM. The peaks at 864, 929, 945, 1107, 1271, 1386, and 2887 cm^{-1} identified in this work can be considered as major indicators to monitor the physio-pathogenesis of articular cartilage. Since *in vivo* Raman spectra have been reported to be collected from human skin, lung, and bone, this technique can therefore advance the diagnostics of AO at an early stage.

Authors Contributions

N'DRE NJ was responsible for the realization of the experiments and the preparation of the manuscript. H. SALEHI supervised the Raman experiments and data analysis. M. MAUMUS prepared the samples for the Raman measurements, and ANURADHA R helped us with the analysis and interpretation of the PCA data. D. NOËL supervised the sample preparation and data analysis. KOFFI-GNAGNE and F. CUISINIER edited the manuscript. All authors contributed to the manuscript with comments and suggestions before publication.

Conflicts of interest

No conflicts of interest are reported.

Author details

N'Dre Jean[1,2]*, Hamideh Salehi[1], Marie Maumus[3], Danièle Noël[3],
Yolande Koffi-Gnagne[2] and Frédéric Cuisinier[1]

1 Bioengineering and Nanosciences Laboratory UM_104, University of Montpellier, France

2 Faculty of Odontostomatology of Abidjan, University Félix Houphouët BOIGNY, Ivory Coast

3 IRMB, University of Montpellier, CHU of Montpellier, France

*Address all correspondence to: njndre08@gmail.com

IntechOpen

References

[1] Kraus VB, Blanco FJ, Englund M, Karsdal MA, Lohmander LS. Call for standardized definitions of osteoarthritis and risk stratification for clinical trials and clinical use. Osteoarthritis Cartilage. 2015;**23**(8):1233-1241

[2] Hunter DJ et al. OARSI Clinical Trials Recommendations: Knee imaging in clinical trials in osteoarthritis. Osteoarthritis Cartilage. 2015;**23**(5):698-715

[3] Mobasheri A, Saarakkala S, Finnilä M, Karsdal MA, Bay-Jensen A-C, van Spil WE. Recent advances in understanding the phenotypes of osteoarthritis. F1000Res. 2019;**8**:268

[4] Henrotin Y. Osteoarthritis in year 2021: Biochemical markers. Osteoarthritis Cartilage. 2022;**30**(2):237-248

[5] Loeser RF, Goldring SR, Scanzello CR, Goldring MB. Osteoarthritis: A disease of the joint as an organ. Arthritis and Rheumatitis. 2012;**64**(6):1697-1707

[6] Tonge DP, Pearson MJ, Jones SW. The hallmarks of osteoarthritis and the potential to develop personalised disease-modifying pharmacological therapeutics. Osteoarthritis and Cartilage. 2014;**22**(5):609-621

[7] Cucchiarini M et al. Basic science of osteoarthritis. Journal of Experimental Otology. 2016;**3**(1):22

[8] Yong CW et al. Knee osteoarthritis severity classification with ordinal regression module. Multimedicine Tools Applied. 2021. DOI: 10.1007/s11042-021-10557-0

[9] Chaudhari AS, Kogan F, Pedoia V, Majumdar S, Gold GE, Hargreaves BA. Rapid knee MRI acquisition and analysis techniques for imaging osteoarthritis. Journal of Magnetic Resonance Imaging. 2020;**52**(5):1321-1339. DOI: 10.1002/jmri.26991

[10] Goodwin M, Workman J, Thambyah A, Vanholsbeeck F. Impact-induced cartilage damage assessed using polarisation-sensitive optical coherence tomography. Journal of the Mechanical Behavior of Biomedical Materials. 2021;**117**:104326

[11] Casal-Beiroa P, González P, Blanco FJ, Magalhães J. Molecular analysis of the destruction of articular joint tissues by Raman spectroscopy. Expert Review of Molecular Diagnostics. 2020;**20**(8):789-802

[12] Mansfield JC, Winlove CP. Lipid distribution, composition and uptake in bovine articular cartilage studied using Raman micro-spectrometry and confocal microscopy. Journal of Anatomy. 2017;**231**(1):156-166

[13] Albro MB et al. Raman spectroscopic imaging for quantification of depth-dependent and local heterogeneities in native and engineered cartilage. NPJ Regeneration Medicine. 2018;**3**(1):1-11

[14] Bergholt MS, Serio A, Albro MB. Raman spectroscopy: Guiding light for the extracellular matrix. Frontier in Bioengineering Biotechnology. 2019;**7**:303

[15] Power L, Wixmerten A, Wendt D, Barbero A, Martin I. Raman spectroscopy quality controls for GMP compliant manufacturing of tissue engineered cartilage. In: Imaging, Manipulation, and Analysis of Biomolecules, Cells, and Tissues XVII. San Francisco, United States; 2019. p. 14

[16] Rieppo L, Saarakkala S, Närhi T, Helminen HJ, Jurvelin JS, Rieppo J. Application of second derivative spectroscopy for increasing molecular specificity of Fourier transform infrared spectroscopic imaging of articular cartilage. Osteoarthritis and Cartilage. 2012;**20**(5):451-459

[17] Takahashi Y. Raman spectroscopy investigation of load-assisted microstructural alterations in human knee cartilage_ Preliminary study into diagnostic potential for osteoarthritis. Journal of the Mechanical Behavior of Biomedical Materials. 2014;**3**:77-85

[18] Kumar R et al. Optical investigation of osteoarthritic human cartilage (ICRS grade) by confocal Raman spectroscopy: A pilot study. Analytical Bioanalytical Chemistry. 2015;**407**(26):8067-8077

[19] Czamara K, Majzner K, Pacia MZ, Kochan K, Kaczor A, Baranska M. Raman spectroscopy of lipids: A review: Raman spectroscopy of lipids. Journal of Raman Spectroscopy. 2015;**46**(1):4-20

[20] Mandair GS, Morris MD. Contributions of Raman spectroscopy to the understanding of bone strength. Bonekey Reports. Jan 2015;**4**:620. DOI: 10.1038/bonekey.2014.115. PMID: 25628882; PMCID: PMC4296861

[21] Bergholt MS et al. Raman Spectroscopy reveals new insights into the zonal organization of native and tissue-engineered articular cartilage. ACS Central Science. 2015;**2**(12):885-895

[22] An R et al. Diagnosis of knee osteoarthritis by OCT and surface-enhanced Raman spectroscopy. Journal of Innovative Optical Health Science. 2022;**2022**:2250027

[23] Athanasiou KA, Darling EM, DuRaine GD, Hu JC, Reddi AH. Articular Cartilage. Second ed. Boca Raton London New York: CRC Press, Taylor & Francis Group; 2017

[24] Das Gupta S et al. Raman microspectroscopic analysis of the tissue-specific composition of the human osteochondral junction in osteoarthritis: A pilot study. Acta Biomaterialia. 2020;**106**:145-155

[25] Mason D, Murugkar S, Speirs AD. Measurement of cartilage sub-component distributions through the surface by Raman spectroscopy-based multivariate analysis. Journal of Biophotonics. 2021;**14**(1):e202000289. DOI: 10.1002/jbio.202000289

[26] Jensen M et al. Multiplexed polarized hypodermic Raman needle probe for biostructural analysis of articular cartilage. Optical Letters. 2020;**45**(10):2890-2893

[27] Pavlou E, Zhang X, Wang J, Kourkoumelis N. Raman spectroscopy for the assessment of osteoarthritis. Annotation Joint. 2018;**3**(83):1-10

[28] Verrier S, Notingher I, Polak JM, Hench LL. In situ monitoring of cell death using Raman microspectroscopy. Biopolymers. 2004;**74**:157. DOI: 10.1002/bip.20063

[29] Zamli Z, Adams MA, Tarlton JF, Sharif M. Increased chondrocyte apoptosis is associated with progression of osteoarthritis in spontaneous Guinea pig models of the disease. International Journal of Molecular Sciences. 2013;**14**(9):9. DOI: 10.3390/ijms140917729

[30] Shaikh R et al. Raman spectroscopy is sensitive to biochemical changes related to various cartilage injuries. Journal of Raman Spectroscopy.

2021;**52**(4):796-804. DOI: 10.1002/jrs.6062

[31] Lim NSJ, Hamed Z, Yeow CH, Chan C, Huang Z. Early detection of biomolecular changes in disrupted porcine cartilage using polarized Raman spectroscopy. Journal of Biomedical Optics. 2011;**16**(1):017003. DOI: 10.1117/1.3528006

[32] Buckwalter JA, Lane NE. Athletics and osteoarthritis. American Journal of Sports Medicine. 1997;**25**(6):873

[33] Safiri S et al. Global, regional and national burden of osteoarthritis 1990-2017: A systematic analysis of the Global Burden of Disease Study 2017. Annals of the Rheumatic Diseases. 2020;**79**(6):819

[34] Villalvilla A, Gómez R, Largo R, Herrero-Beaumont G. Lipid transport and metabolism in healthy and osteoarthritic cartilage. IJMS. 2013;**14**(10):20793

[35] Gaifulina R et al. Intra-operative Raman spectroscopy and ex vivo Raman mapping for assessment of cartilage degradation. Clinical Spectroscopy. 2021;**3**:100012

[36] Papathanasiou I, Anastasopoulou L, Tsezou A. Cholesterol metabolism related genes in osteoarthritis. Bone. 2021;**152**:116076

[37] Meng H, Jiang L, Song Z, Wang F. Causal associations of circulating lipids with osteoarthritis: A bidirectional mendelian randomization study. Nutrients. 2022;**14**(7):7. DOI: 10.3390/nu14071327

[38] Bergholt MS, Albro MB, Stevens MM. Online quantitative monitoring of live cell engineered cartilage growth using diffuse fiber-optic Raman spectroscopy. Biomaterials. 2017;**140**:128-137

[39] Bergholt MS et al. Simultaneous fingerprint and high-wavenumber fiber-optic Raman spectroscopy enhances real-time in vivo diagnosis of adenomatous polyps during colonoscopy. Journal of Biophotonics. 2016;**9**(4):333-342. DOI: 10.1002/jbio.201400141

[40] Kandel S, Querido W, Falcon JM, Reiners DJ, Pleshko N. Approaches for in situ monitoring of matrix development in hydrogel-based engineered cartilage. Tissue Engineering Part C: Methods. 2020;**26**(4):225-238

[41] Esmonde-White KA, Esmonde-White FWL, Morris MD, RoesslerBJ.Fiber-opticRamanspectroscopy of joint tissues. Analyst. 2011;**136**(8):1675

[42] Gao T, Boys AJ, Zhao C, Chan K, Estroff LA, Bonassar LJ. Non-destructive spatial mapping of glycosaminoglycan loss in native and degraded articular cartilage using confocal raman microspectroscopy. Frontiers in Bioengineering Biotechnology. 2021;**9**:744197